

Activation of Different Heterodimers of TLR2 Distinctly Mediates Pain and Itch

Ting-Ting Wang,^{a,c,d†} Xian-Yun Xu,^{a,b,c†} Wei Lin,^e Dan-Dan Hu,^{a,b,c} Wu Shi,^{a,b,c} Xin Jia,^{a,b,c} Hui Wang,^a Ning-Jing Song,^d Yu-Qiu Zhang^e and Ling Zhang^{a,b,c*}

^a The First Rehabilitation Hospital of Shanghai, Tongji University School of Medicine, Shanghai 200090, China

^b Key Laboratory of Spine and Spinal Cord Injury Repair and Regeneration of Ministry of Education, Orthopaedic Department of Tongji Hospital, School of Medicine, Tongji University, Shanghai, 200065, China

^c Department of Anatomy and Histology, Tongji University School of Medicine, Shanghai 200092, China

^d Department of Dermatology, Tongren Hospital Shanghai Jiao Tong University School of Medicine Shanghai 200336, China

^e State Key Laboratory of Medical Neurobiology and MOE Frontiers Center for Brain Science, Department of Translational Neuroscience, Institutes of Brain Science, Fudan University, Shanghai 200032, China

Abstract—Toll-like receptors (TLRs) have been implicated in pain and itch regulation. TLR2, a TLR family member that detects microbial membrane components, has been implicated in pathologic pain. However, the role of TLR2 in pruritic and nociceptive responses has not been thoroughly investigated. In this study, we found that TLR2 was expressed in mouse dorsal root ganglia (DRG) and trigeminal ganglia (TG) neurons. Itch and pain behaviors, including histamine-dependent and histamine-independent acute itching, acetone/diethyl ether/water and 2,4-dinitrofluorobenzene-induced chronic itching and inflammatory pain, were largely attenuated in TLR2 knockout (KO) mice. The TLR2 agonist Pam3CSK4, which targets TLR2/1 heterodimers, evoked pain and itch behavior, whereas lipoteichoic acid (LTA) and zymosan, which recognize TLR2/6 heterodimers, produced only pain response. The TLR2 agonist-induced nociceptive and pruritic behaviors were largely diminished in transient receptor potential vanilloid 1 (TRPV1) and transient receptor potential ankyrin 1 (TRPA1) KO mice. Finally, Pam3Csk4 and zymosan increased the $[Ca^{2+}]_i$ in DRG neurons from wild-type mice. However, the enhancement of $[Ca^{2+}]_i$ was largely inhibited in the DRG neurons from TRPV1 and TRPA1 KO mice. Our results demonstrate that TLR2 is involved in different itch and pain behaviors through activating TLR1/TLR2 or TLR6/TLR2 heterodimers via TRPV1 and TRPA1 channels. © 2020 IBRO. Published by Elsevier Ltd. All rights reserved.

Key words: TLR2, pain, itch, TRPV1, TRPA1.

INTRODUCTION

Toll-like receptors (TLRs) recognize pathogen-associated molecular patterns (PAMPs) and danger-associated molecular patterns (DAMPs), initiating signals in innate and adaptive immunity (Akira et al., 2006). To date, more than 10 TLRs have been found in humans and mice (Kawai and Akira 2010). These receptors are expressed on cell or organelle membranes to sense different molecular patterns of viruses, bacteria, mycobacteria, fungi and parasites, participating in the immune response. Increas-

ing evidence has shown that TLRs in the nervous system mediate pain and itch sensations (Liu et al., 2012b; Lacagnina et al., 2018). For example, TLR2, TLR4, TLR5, TLR7, TLR8 and TLR9 have been reported to induce neuropathic pain or spinal neuron plasticity (Kim et al., 2007; Christianson et al., 2011; Xu et al., 2015; Zhang et al., 2018; Luo et al., 2019). Particularly, recent studies have also demonstrated that TLR3, TLR4, and TLR7, which are expressed in a subset of pruriceptive and nociceptive neurons in the dorsal root ganglia (DRG) and trigeminal ganglia (TG), contribute to the processing of itch sensation (Liu et al., 2010; Liu et al., 2012a; Liu et al., 2016).

TLR2, a member of the TLR family, is expressed on the cell membrane for the detection of microbial membrane components and has been implicated in neuropathic pain processes (Kim et al., 2007; Kim et al., 2011a; Lim et al., 2013). Clinical data have indicated that TLR2 is highly expressed in the skin of individuals with chronic pruritic dis-

*Corresponding author.

E-mail address: lzhang0808@tongji.edu.cn (L. Zhang).

† TT.W., XY.X contributed equally to this work.

Abbreviations: CGRP, calcitonin gene-related peptide; DAMPs, danger-associated molecular patterns; DNFB, 2,4-dinitrofluorobenzene; DRG, dorsal root ganglia; GAPDH, glyceraldehyde-3-phosphate dehydrogenase; KO, knockout; LTA, lipoteichoic acid; PAMPs, pathogen-associated molecular patterns; TG, trigeminal ganglia; TLRs, toll-like receptors.

eases such as atopic dermatitis and psoriasis (Panzer et al., 2014). However, whether TLR2 is involved in the regulation of pruritus has not been reported.

Among TLR family members, TLR2 recognizes the widest range of PAMPs derived from bacteria, fungi, parasites and viruses (Kawai and Akira 2010). Upon stimulation, while most of the other TLRs form homodimers between themselves, TLR2 mainly forms heterodimers with TLR1 and TLR6 on the cell membrane (Triantafilou et al., 2007; Oosting et al., 2011). The specificity of the TLR2 ligand is modulated by its heterodimeric partner, and different TLR2 agonists have been implicated in different signaling pathways and cell functions (Triantafilou et al., 2006; Oliveira-Nascimento et al., 2012; Vaisid and Kosower 2013). However, whether activation of different TLR2 heterodimers induces distinct nociceptive/pruriceptive behaviors has not been demonstrated.

In the present study, we first revealed that TLR2 is expressed in small- to medium-sized primary sensory neurons in the DRG and TG and is primarily coexpressed with IB4 and slightly less with calcitonin gene-related peptide (CGRP), TRPV1 and TRPA1. Then, we demonstrated that TLR2 is involved in distinct itch and pain behaviors through activating TLR2/TLR1 or TLR2/TLR6 heterodimers. Finally, we demonstrated that itch and pain behaviors and the increased $[Ca^{2+}]_i$ in DRG neurons induced by TLR2 agonists depend on TRPV1 and TRPA1 channels.

EXPERIMENTAL PROCEDURES

Animal

C57BL/6 mice were purchased from SLAC Laboratory Animal Company (Shanghai, China). All mice, including TLR2 KO, TRPA1 KO and TRPV1 KO mice, were housed at a controlled temperature ($22 \pm 2^\circ\text{C}$) and humidity (60–80%) under a 12-h/12-h light/dark cycle and provided food and water *ad libitum*. All experiments were performed in accordance with the guidelines for animals used in biological studies of Tongji University and were approved by the Animal Study Committee at Tongji University School of Medicine, Shanghai, China.

Behavior tests

A cheek model was established to differentiate itch and pain behavior (Shimada and LaMotte, 2008). The unilateral cheeks of mice were shaved one day before the intradermal injection of pruritogens or algogens, and wiping and scratching behavior were then recorded within 30 min after the administration of reagents. The 2,4-dinitrofluorobenzene (DNFB) mouse model was established as a chronic itch model as described previously (Zhang et al., 2014; Huang et al., 2018). The mice received repeated skin painting with 150 μl of 0.15% DNFB (Sigma-Aldrich, St Louis, MO) in acetone at the shaved nape 4 times in 2 weeks. Spontaneous itching behavior was observed at 1, 3, 5, 7, and 14 days after the final DNFB administration. Scratch behaviors were assessed for 30 min at that same time of day.

The acetone/diethyl ether/water (AEW)-induced itch model was also established as a mouse model of chronic dry skin itch as described previously (Zhou et al., 2017). The mice were shaved at the nape one day before the start of the experiment. Cotton soaked with a mixture of acetone and diethyl ether (1:1) was applied to the shaved area for 15 seconds, followed immediately by application of distilled water-soaked cotton for 45 seconds, twice per day (10:00 AM and 8:00 PM) for 1 week. Spontaneous scratching behavior was evaluated for 1 h at 1, 3, 5, and 7 days after the final administration.

An inflammatory pain model was created by injection of complete Freund's adjuvant (CFA, 20 μl) and 5% formalin into the mouse's hind paw (20 μl). Mechanical and thermal pain sensitivity were measured before and after the mice were treated with CFA or formalin.

All scratch behaviors were recorded using a video camera (SONY HDR-CX240), and the counting and analysis were performed by an experimenter blinded to the treatment conditions.

For the pain behavior test, mice were placed on the shelf for 30 min every day for three days before the experiment, and mechanical allodynia was measured by the "up-down" method (Chaplan et al., 1994). After adaptation, the mouse hind paw was stimulated by Von Frey filaments, and reflex, licking and flinching were considered positive reactions. Heat hyperalgesia was tested using the Plantar Analgesia Meter (Model 400, IITC Life Science). The latency of paw withdrawal after the stimulation of radiant heat was calculated. For the tail reflex test, the mice were gently handled and immobilized. The final third of a mouse's tail was placed in hot water at 48 $^\circ\text{C}$, 50 $^\circ\text{C}$ and 52 $^\circ\text{C}$. The latency of the tail flap out of the hot water was calculated. To prevent tissue damage, the tail was exposed to hot water for no more than 20 seconds.

Drug administration

The TLR2 agonists Pam3Csk4, lipoteichoic acid (LTA) and zymosan (Sigma-Aldrich) were dissolved in PBS or saline. Pam3Csk4 (1 μg , 3 μg , 10 μg in 10 μl), LTA (10 μg , 50 μg and 100 μg in 10 μl) and zymosan (30 μg and 300 μg in 10 μl) were intradermally injected into the cheek through a 30-gauge needle. Control mice received an equal volume of PBS or saline only.

Immunohistochemistry

Mice were anesthetized by the perfusion of sodium pentobarbital in PBS through the ascending aorta, followed by 4% paraformaldehyde in 0.1 M phosphate buffer (pH 7.4). After perfusion, the cervical segments of the DRG and TG were removed and postfixed for 4 h. Samples were cut into 14- μm -thick frozen sections on a cryostat and then processed for immunofluorescence. The following primary antibodies were used: rabbit anti-TLR2 antibody (1:100, Biorbyt, Cambridge, UK), mouse anti-TLR2 antibody (1:100, Abcam, Cambridge, UK), mouse anti-TLR1 antibody (1:100, Santa Cruz, California, USA), rabbit anti-TLR6 antibody (1:400, Bioss, Beijing, China), mouse anti-NF200 antibody (1:500, Abcam Cambridge, UK), goat anti-CGRP antibody (1:500,

Abcam), anti-IB4-FITC antibody (1:1000, Sigma-Aldrich), rabbit anti-TRPA1 antibody (1:500, Abcam, Cambridge, UK) and goat anti-TRPV1 antibody (1:200, Santa Cruz, Dallas, TX). The sections were incubated with the primary antibodies overnight at 4 °C, followed by incubation with biotin-conjugated horse anti-goat or horse anti-mouse antibodies (1:500, Vector laboratories, Burlingame, CA) for 2 h and with Cy3-conjugated streptavidin (1:1000, Jackson Immuno-Research, West Grove, PA) for 1 h at room temperature. For double immunofluorescence, sections were incubated with a mixture of rabbit polyclonal and mouse or goat monoclonal primary antibodies, followed by a mixture of Alexa Fluor 488- and biotin-conjugated horse anti-rabbit IgG and Cy3-conjugated streptavidin. DRG and TG sections were photographed on a Zeiss Imager M2 (Carl Zeiss Jena, Germany) with a 20× objective and captured digitally on a uniform scale using Zeiss Axio Vision Rel.4.8. All images were made into figures using Adobe Photoshop (Adobe Systems Incorporated, San Jose, CA), with only minor adjustments to the contrast and brightness settings being applied if necessary. For quantitative analysis of TLR2-positive neurons in the DRG, the area of TLR2-positive cells was analyzed via ImageJ.

Quantitative real-time RT-PCR

The bilateral cheeks of mice were shaved one day prior to the bilateral intradermal injection of Pam3CSK4 (10 µg in 10 µl), LTA (100 µg in 10 µl) or zymosan (300 µg in 10 µl) into the cheeks. Mice in the control group were injected with an equal amount of PBS or normal saline. The mice were killed by acute decapitation 30 min later, and bilateral TGs were rapidly separated on ice by sterilized instruments. Total RNA was extracted and reverse transcribed to synthesize the first-strand cDNA using the Fast Quant RT Kit (Tiangen, Beijing, China). The primer sequences were as follows: TLR1 forward and reverse, GTGTCCGTCAGCACTAC and GCTTCAGATTCTTTC CA; TLR2 forward and reverse, TCGTTCATCTCTCTGG AGCATC and TTGACGCTTTGTCTGAGGTT; TLR6 forward and reverse, TAGTTTAGAGTGTGGTGG and ATCAGGTTAGTGGGTAT; TRPA1 forward and reverse, GGCAATGTGGAGCAATAGCG and CAATAAGCTGC CCAAAGGTC; and TRPV1 forward and reverse, AGCTGCAGCGAGAGCCATCACCA and ATCCTTGCC GTCCGGCGTGA. Super Real Premix Plus (SYBR Green, Tiangen) was used in the PCR. Real-time PCR liquid was prepared, and the reaction conditions were set according to the manufacturer's instructions. Glyceraldehyde-3-phosphate dehydrogenase (GAPDH) served as an internal control. The melting curve was used to evaluate the reliability of the PCR results. Cycle threshold (Ct) values (inflection point of the amplification curve) were determined, and the relative expression levels of target genes were calculated using the $2^{-\Delta\Delta Ct}$ method.

Calcium imaging

The DRG neurons acutely isolated from spinal L3–L5 segments were loaded with 1 µM fura-2 AM (DoJinDo

Laboratories) for 1 h and washed and incubated with a DRG external solution containing the following (in mM): 150 NaCl, 5 KCl, 2.5 CaCl₂·H₂O, 1 MgCl₂, 10 HEPES, 10 Glucose, pH 7.4. The neurons were observed on a microscope (Olympus IX51) with a 40 × UV flour oil-immersion objective lens. Images of the DRG neurons were captured every 1 second with a cooled Digital CMOS camera (monochromators; Till Polychrome IV) at excitation wavelengths of 340 nm and 380 nm. The images were analyzed by SimplePCI (Compix). The ratio of the fluorescence intensity at the two excitation wavelengths (340/380) represented an estimate of the changes in the [Ca²⁺]_i.

Quantification and statistics

Quantification and statistics Data are expressed as the mean ± SEM or the median in box-plots where the bottom and the top of the box are the first and third quartiles, respectively, and the whiskers above and below the box indicate the 95th and 5th percentiles. Differences between two groups were compared using 2-tailed Student's *t* test. One-way ANOVA followed by a Fisher post hoc or Bonferroni's post hoc test were used to evaluate the differences among multiple groups. Differences with *P* < 0.05 were considered statistically significant.

RESULTS

TLR2 is expressed in small- to medium-sized primary sensory neurons in the DRG and TG

We first measured the expression of TLR2 in primary sensory neurons in the DRG and TG using immunofluorescence. TLR2 was mainly expressed in small (< 300 µm²) and medium (300–700 µm²) DRG (91.23%, 1644 in 1802) and TG (86.9%, 2112 in 2430) neurons in mice (Ichikawa et al., 2004; Ruscheweyh et al., 2007; Towne et al., 2009) (Fig. 1A, C, E, F). TLR2 KO mice showed few TLR2-positive neurons in the DRG and TG (Fig. 1B, D). Double immunostaining experiments further showed that TLR2 was coexpressed with NF200 (13.23%, 166/1258), CGRP (24.27%, 168/702), IB4 (45.52%, 581/1319), TRPV1 (22.71%, 294/1317) and TRPA1 (33.78%, 249/737) in DRG neurons (Fig. 2A–J, K). In TG neurons, the coexpression of TLR2 with NF200 (18.11%, 219/1250), CGRP (27.44%, 477/1588), IB4 (48.19%, 308/640) and TRPV1 (21.69%, 331/1552) was comparable to that in DRG neurons (Fig. 2L). These data showed that most TLR2 is expressed in peptidergic, nonpeptidergic, TRPV1- and TRPA1-positive primary sensory neurons, implicating the possible role of TLR2 in the modulation of pain and itch sensation.

TLR2 KO mice exhibit normal pain sensitivity but attenuated formalin- and CFA-induced inflammatory pain

To examine the function of TLR2 in the regulation of nociception, pain behaviors were examined in TLR2 KO mice. First, thermal and mechanical pain thresholds and

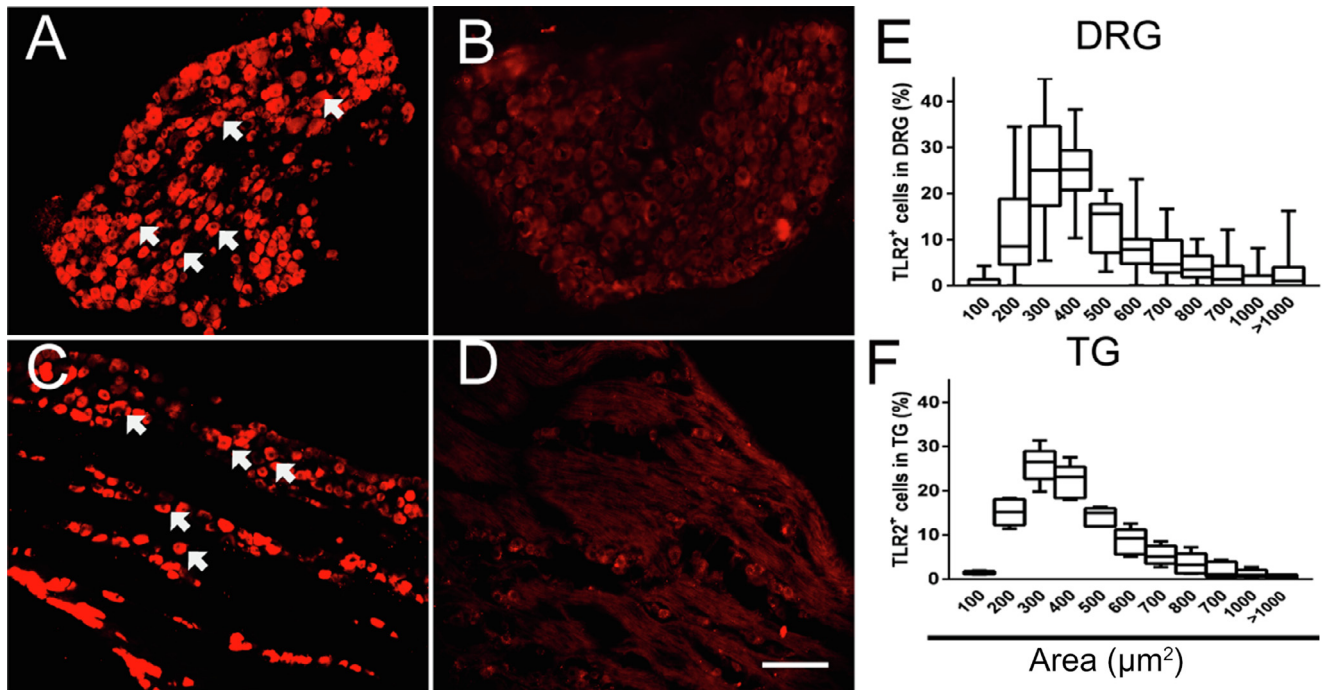


Fig. 1. TLR2 is expressed in DRG and TG neurons. (A–B) TLR2 was expressed in DRG neurons of wild-type (A) and TLR2 KO (B) mice. (C–D) TLR2 was expressed in TG neurons of wild-type (C) and TLR2 KO (D) mice. (E–F) Distributions of TLR2 in DRG (E) and TG (F) neurons of different sizes. The arrows indicate the TLR2-positive neurons. N = 5–7 for each group. Bar = 50 μm.

tail reflex were measured, and no significant differences were observed between the TLR2 KO mice and the wild-type controls (Fig. 3A–C). However, both CFA-induced inflammatory pain behavior (Fig. 3D, E) and the formalin-induced 1st and 2nd phases of spontaneous pain (Fig. 3F, G) were robustly reduced in TLR2 KO mice. The data suggested that TLR2 does not affect basal pain sensitivity but mediates the pathological pain behavior caused by inflammation.

TLR2 is required for both histamine-dependent and histamine-independent acute itch as well as AEW- and DNFB-induced chronic itch

To investigate whether TLR2 is involved in the regulation of itch sensation, we measured a series of pruritic behaviors in TLR2 KO mice and compared them with those in the wild-type controls. First, histamine and chloroquine were injected into the necks of mice to detect acute histamine-dependent and histamine-independent pruritus. Both histamine- and chloroquine-induced scratch behaviors were significantly decreased in TLR2 KO mice (Fig. 4A, B). Further chronic itch experiments showed that the spontaneous itch behavior induced by AEW and repeated DNFB treatment were significantly diminished in TLR2 KO mice (Fig. 4 C, D). These results indicated that TLR2 is extensively involved in acute and chronic itch responses.

Different TLR2 agonists evoke distinct pain and itch behaviors

Upon stimulation, TLR2 combines with TLR1 or TLR6 to form heterodimers and is expressed on the cell

membrane (Takeda et al., 2002; Kawai and Akira 2011). TLR1/TLR2 can be activated by triacyl lipopeptides such as Pam3CSK4, whereas TLR6/TLR2 is activated by diacyl lipopeptides such as LTA and a component of the yeast cell wall, zymosan (Kang et al., 2009; Oliveira-Nascimento et al., 2012). To determine whether different TLR2 agonists induce distinct nociceptive/pruritic behaviors, we used a cheek model to observe the wiping and scratching behavior after injection of Pam3CSK4, LTA and zymosan into the cheeks of mice. Pam3CSK4 caused dose-dependent scratching and wiping in mice, and both behaviors were dramatically reduced in TLR2 KO mice compared with wild-type mice (Fig. 5A–C). In contrast, LTA and zymosan produced dose-dependent wiping behavior, and the scratching behavior was maintained at a low level and did not change as the dose of LTA or zymosan increased. The wiping behavior induced by LTA and zymosan was also significantly diminished in TLR2 KO mice (Fig. 5 D–I).

TLR2 mediated pain and itch behavior through activation of TRPA1 and TRPV1 channels

TRPA1 and TRPV1 are expressed by pruriceptive and nociceptive DRG neurons and regulate acute and chronic pain and itching (Kim et al., 2008; Kim et al., 2011b; Akiyama and Carstens 2013; Moore et al., 2018). Previous reports showed that TLR3, TLR4 and TLR7 induce itching and pain mainly by TRPA1 and TRPV1 (Liu et al., 2010; Liu et al., 2012a; Hyunjung Min et al., 2014; Park et al., 2014). We used real-time PCR to detect the expression of TRPA1 and TRPV1 in the TG after intradermal injection of Pam3CSK4, LTA and zymosan into the cheek. The mRNA expression levels

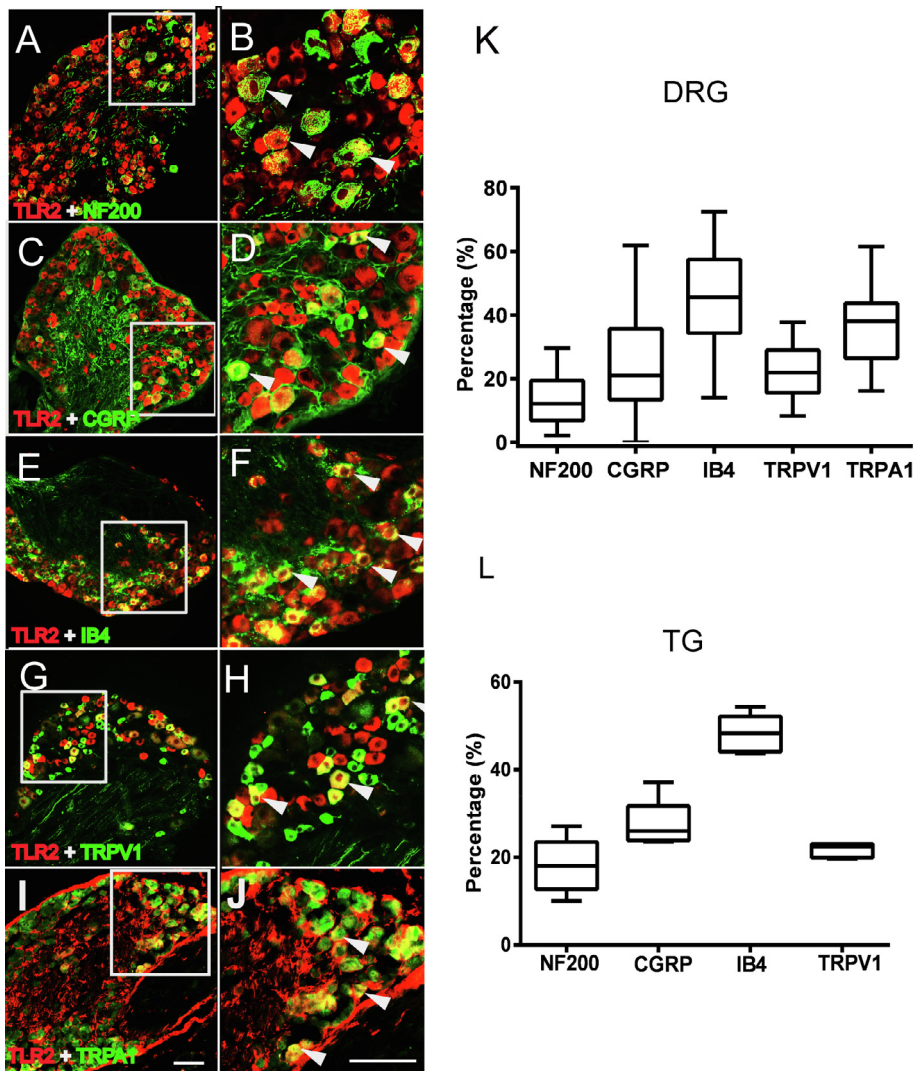


Fig. 2. Colabeling of TLR2 with NF200, CGRP, IB4, TRPV1 and TRPA1 in mouse DRG and TG neurons. (A–J) TLR2 colocalized with NF200 (A, B), CGRP (C, D), IB4 (E, F), TRPV1 (G, H) and TRPA1 (I, J) in DRG neurons. B, D, F, H, J are high magnifications of A, C, E, G, I. (K–L) The percentage of TLR2 colocalization with NF200, CGRP, IB4, TRPV1 and TRPA1 in DRG (K) and TG (L) neurons. The arrowheads indicate colocalized TLR2 neurons. N = 5; Bar = 50 μ m.

of TLR2, TRPV1 and TRPA1 in the TG were robustly upregulated by all the TLR2 agonists used (Fig. 6 A–C). Notably, Pam3CSK4 increased the mRNA expression of TLR1 and TLR2 but not TLR6 (Fig. 6A), whereas LTA and zymosan enhanced the mRNA expression of TLR6 and TLR2 but not TLR1 in the TG (Fig. 6 B, C). We also examined the coexpression of TLR2, TLR1 and TLR6 in DRG neurons. The immunostaining results showed that both TLR1 and TLR6 were partially coexpressed with TLR2 (Fig. 6 D, E). In addition, TLR1 and TLR6 were also coexpressed in DRG neurons to a certain degree (Fig. 6 F).

Furthermore, the scratching and wiping behavior induced by Pam3CSK4 and the wiping behavior induced by LTA and zymosan were dramatically decreased in both TRPV1 and TRPA1 KO mice (Fig. 7 A, B). To further verify that TRPV1 and TRPA1 are involved in TLR2-induced pain and itch behaviors, calcium imaging in DRG neurons was conducted. Pam3CSK4 and

zymosan, which activates TLR2/1 and TLR2/6 respectively, increased the $[Ca^{2+}]_i$ in DRG neurons of wild-type mice. However, the increase in $[Ca^{2+}]_i$ was blocked in the TRPV1 KO and TRPA1 KO mice (Fig. 7 C–E). These results indicate that TLR2-induced pain and itching may due to the activation of downstream TRPV1 and TRPA1 to induce calcium influx in DRG neurons.

DISCUSSION

Increasing studies have shown that TLRs are expressed in not only immune cells but also neuronal and nonneuronal cells in the nervous system, contributing to inflammatory diseases. TLRs have been found in various types of cells, including glial cells and neurons, in the central and peripheral nervous systems. Recently, TLR3, 4, and 7 have been reported to be expressed in a subset of prurceptive/nociceptive DRG and TG neurons in mice (Liu et al., 2010; Liu et al., 2012a; Taves and Ji 2015). Moreover, TLR3, 4, 7, and 9 were also detected in human TG neurons (Wadachi and Hargreaves 2006; Qi et al., 2011). In the present study, we found that TLR2 was expressed in small- to medium-sized TG and DRG mouse neurons and coexpressed with IB4, CGRP, TRPV1 and TRPA1 but not GFAP in the DRG (data not shown), providing a morphological basis for the contribution of TLR2 to pain and itch sensations.

Recently, an increasing number of TLRs has been implicated in the regulation of pathological pain (Liu et al., 2012b; Bruno et al., 2018; Lacagnina et al., 2018). First, TLR4 in DRG and TG neurons contributes to dental and neuropathic pain (Wadachi and Hargreaves 2006; Wu et al., 2015). TLR4 in the spinal cord also mediates the transition to persistent mechanical hypersensitivity after the resolution of inflammation in arthritis (Christianson et al., 2011). Furthermore, lipopolysaccharide (LPS), the TLR4 agonist, exacerbates postincisional pain (Kawano et al., 2016). Second, TLR5, which is coexpressed with NF200 in large DRG neurons, mediates mechanical allodynia in neuropathic pain (Xu et al., 2015). Third, TLR8 in mouse DRG neurons and its endogenous ligand miR-21 contribute to neuropathic pain (Zhang et al., 2018). A very recent study revealed sex-dimorphic macrophage TLR9

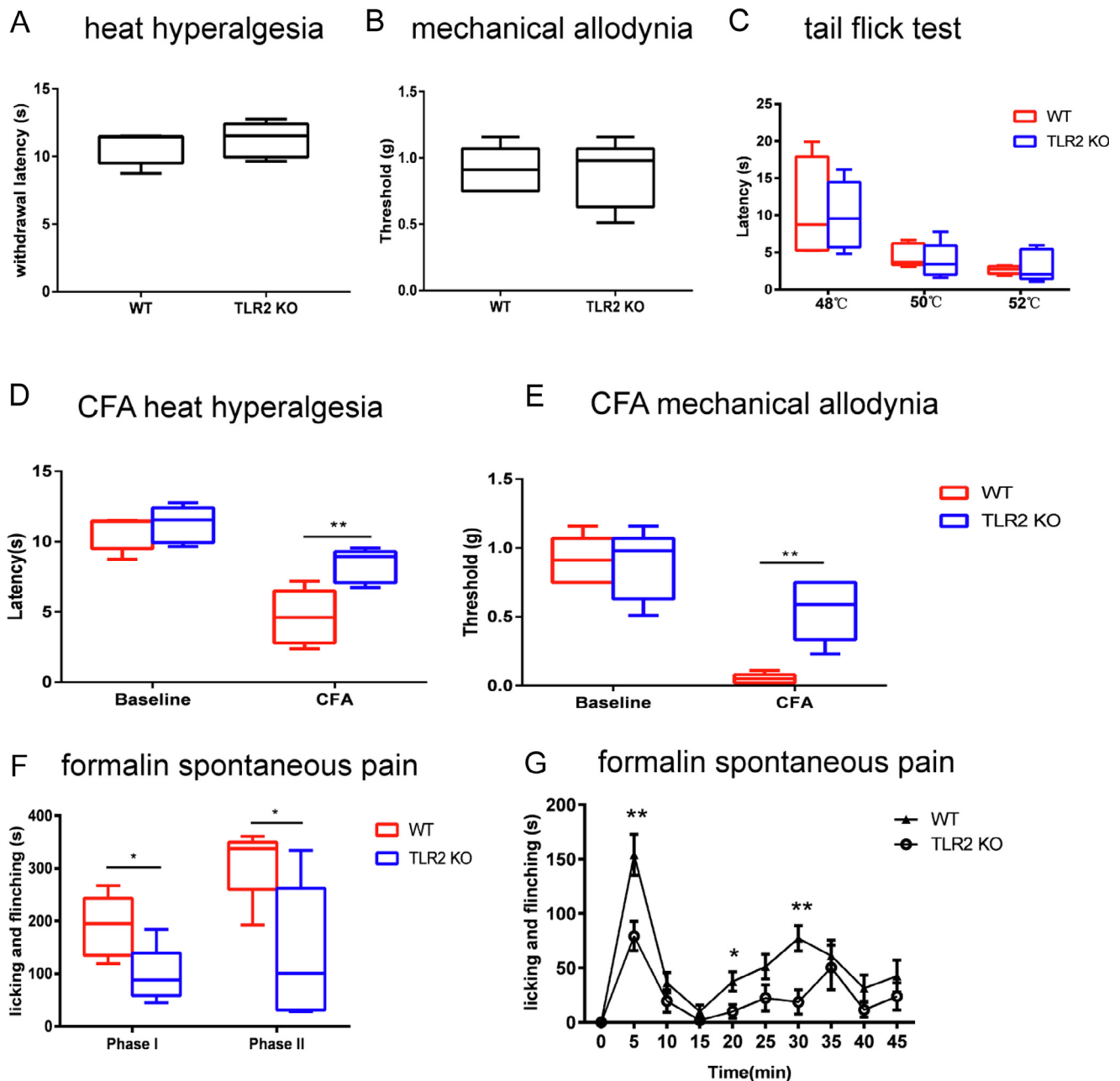


Fig. 3. TLR2 does not affect the basal pain threshold but mediates inflammatory pain. (**A–C**) Acute heat hyperalgesia (**A**), mechanical allodynia (**B**) and tail reflex (**C**) were measured in TLR2 KO and wild-type mice. The TLR2 KO mice showed heat pain (**A**, **C**) and mechanical pain (**B**) thresholds that were comparable to those of wild-type mice. (**D–E**) TLR2 KO mice exhibited attenuated mechanical allodynia (**E**) and heat hyperalgesia (**D**) induced by CFA. (**F–G**) The 1st and 2nd spontaneous pain phases induced by formalin were dramatically reduced in TLR2 KO mice. N = 5–7 for each group. *P < 0.05; **P < 0.01.

signaling in chemotherapy-induced neuropathic pain (Luo et al., 2019). Although TLR2 has been reported to mediate neuropathic pain (Kim et al., 2007; Kim et al., 2011a), its involvement in inflammatory pain has not been reported. According to our present study, TLR2 does not affect the baseline heat and mechanical pain sensitivity but mediates inflammatory pain behavior, as CFA-induced heat and mechanical- and formalin-induced spontaneous licking and flinching behavior were dramatically reduced in TLR2 KO mice.

Increasing evidence has shown that TLRs mediate the transmission and modulation of itching (Liu et al., 2012a; Liu et al., 2012b; Hyunjung Min et al., 2014; Liu and Ji 2014). TLR3 and TLR7 in small DRG neurons play an important role in regulating itch sensation and the excitation of DRG neurons (Liu et al., 2010; Liu et al., 2012a). TLR4 on sensory neurons enhances histamine-induced itch signal transduction by potentiating TRPV1 activity (Hyunjung Min et al., 2014) and is important for spinal astrocyte activation and chronic itching (Liu et al.,

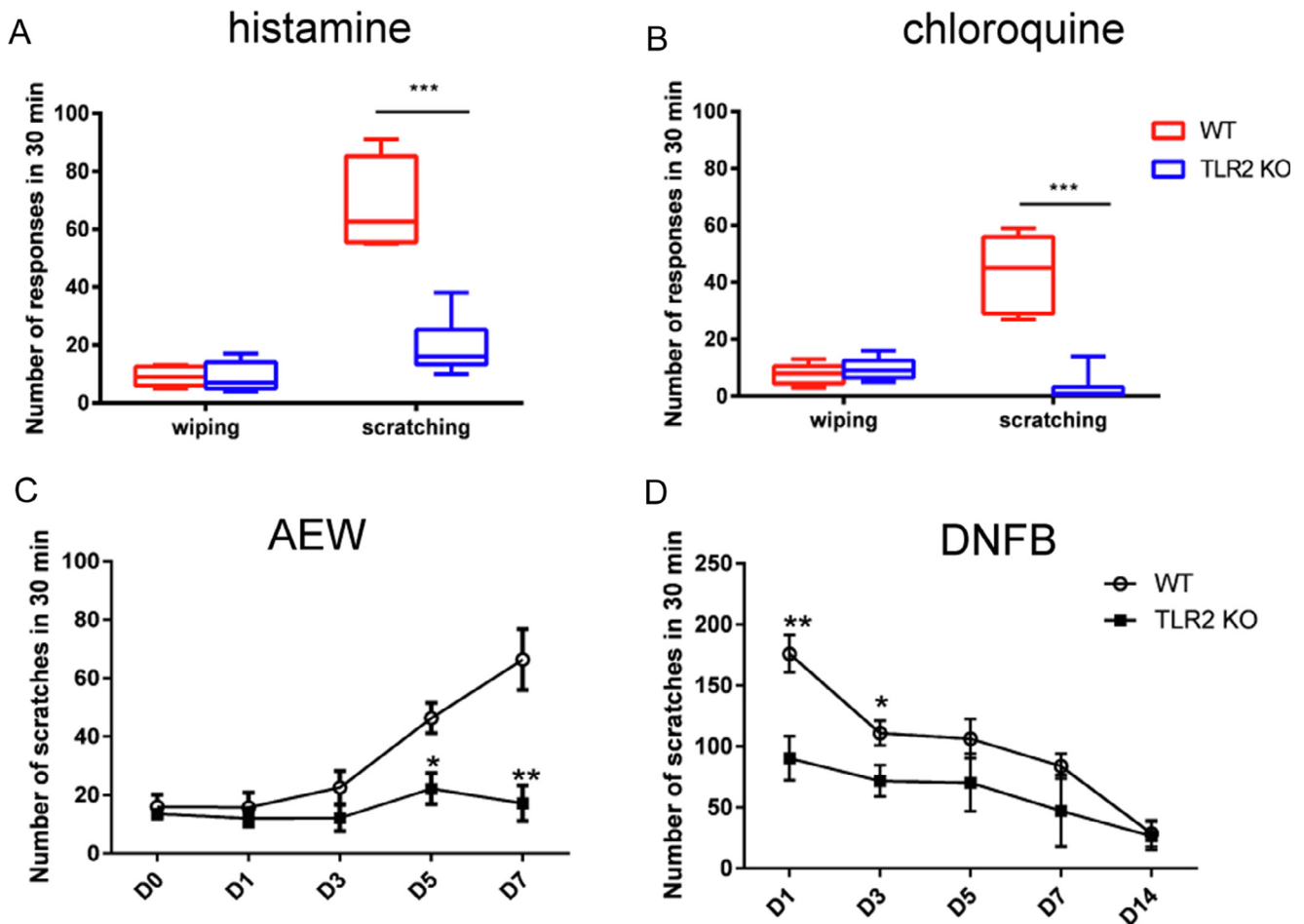


Fig. 4. TLR2 mediates acute and chronic itching. **(A–B)** Histamine- and chloroquine-induced scratching behaviors were dramatically decreased in TLR2 KO mice compared with wild-type mice. **(C–D)** Spontaneous scratching in AEW- and DNFB-repeated painting chronic itch models was attenuated in TLR2 KO mice compared with wild-type mice. N = 5–7 for each group. *P < 0.05; **P < 0.01; ***P < 0.001.

2016). In our study, TLR2 was shown to play roles in various acute and chronic itch behaviors, including histamine-dependent and histamine-independent acute itching as well as DNFB- and AEW-induced chronic itching. Because many clinical reports have demonstrated the contributions of TLR2 to various inflammatory skin diseases, such as AD, contact dermatitis, and psoriasis (Ionescu et al., 2011; Panzer et al., 2014; Sakamoto et al., 2016), our study may implicate a role for TLR2 in itch responses caused by inflammatory skin diseases.

TLR family members recognize different ligands (Alexopoulou et al., 2002). For example, TLR3 and TLR7/8 detect double- and single-stranded RNAs, TLR5 recognizes flagellin, and TLR9 reacts with CpG DNA (Kawai and Akira 2010; Liu and Ji 2014). Although TLR2 and TLR4 both recognize bacterial cell wall components, TLR4 recognizes Gram-negative bacterial cell wall components, such as LPS, and TLR2 recognizes lipoprotein and phospholipids of the bacterial wall of Gram-positive bacteria. While other TLRs, including TLR4, form homodimers upon stimulation, TLR2 forms heterodimers with TLR1 or TLR6, and these different heterodimers have different agonists (Takeda et al., 2002; Takeuchi et al., 2002; Jin et al., 2007). Because the molecular

structures of these agonists are diverse, TLR2 likely has different capabilities to react with different agonists (Zahringer et al., 2008), consequently resulting in the activation of different downstream pathways (Vaisid and Kosower 2013). The TLR1/2 complex binds to triacyl lipopeptides such as Pam3CSK4, while the TLR2/6 complex interacts with diacyl lipopeptides such as LTA and a component of the yeast cell wall, zymosan (Takeuchi and Akira 2001; Alexopoulou et al., 2002; Takeuchi et al., 2002; Yamamoto et al., 2002; Jin et al., 2007; Kang and Lee, 2011). In the present study, Pam3CSK4, the TLR1/2 agonist, induced scratching and wiping behaviors, while LTA and zymosan, agonists of TLR2/6, only caused pain behaviors in mice. In addition, both the scratching and wiping behaviors induced by Pam3CSK4 and the wiping behavior induced by LTA and zymosan were significantly reduced in TLR2 KO mice. The results suggested that activation of TLR2 may induce different pruritic or nociceptive behaviors through activating different TLR2 heterodimers via TLR1 or TLR6.

Apart from their extensive involvement in the nociceptive response, TRPV1 and TRPA1 also contribute to itch sensation (Moore et al., 2018). According to a recent study, TRPV1 plays an important role in

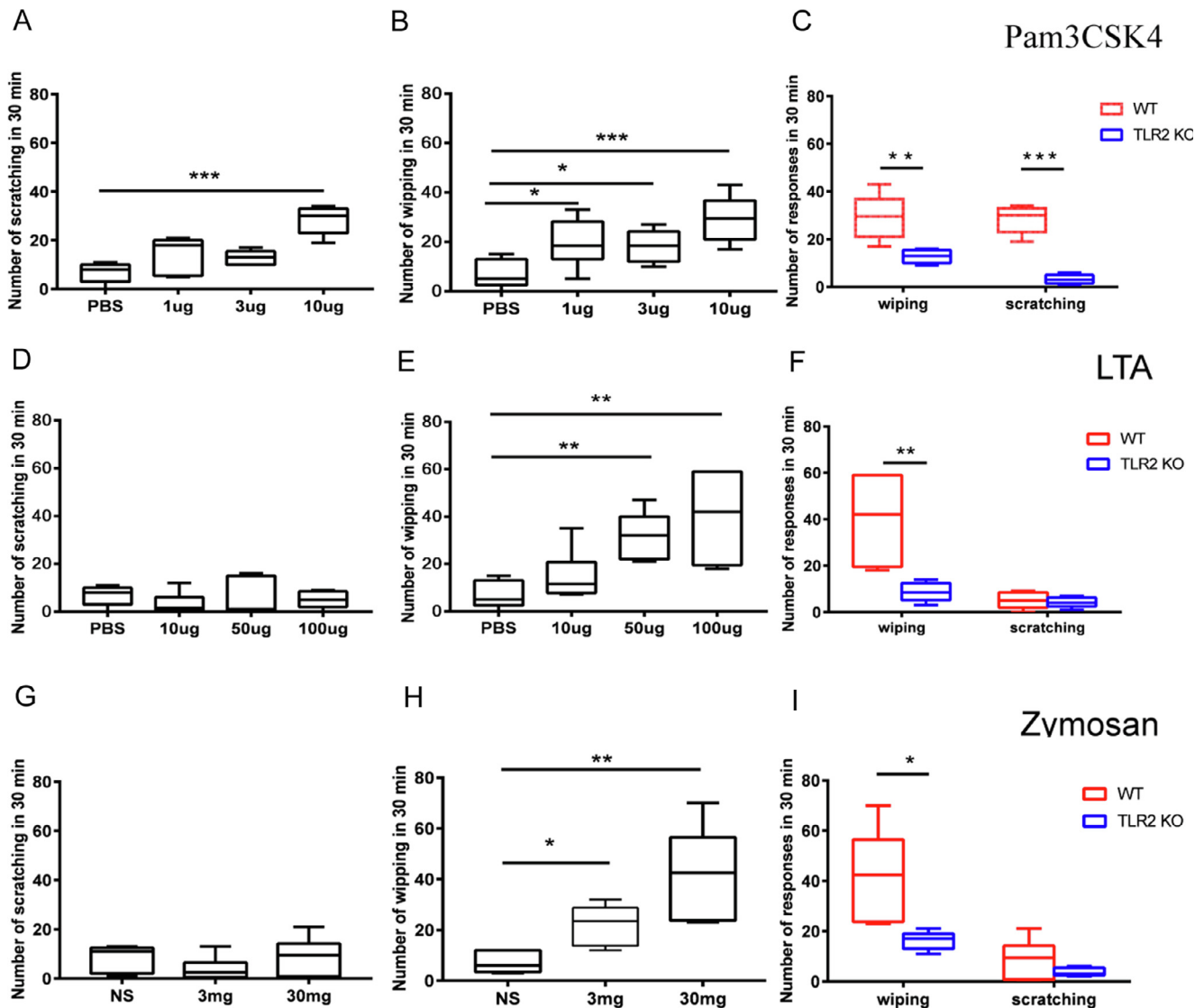


Fig. 5. Different TLR2 agonists evoke distinct pain and itch behaviors. (A–C) Pam3CSK4 induced dose-dependent scratching (A) and wiping (B); both the scratching and wiping were diminished in TLR2 KO mice compared with wild-type mice (C). (D–F) LTA induced dose-dependent wiping (E) but not scratching (D); the wiping was reduced in TLR2 KO mice (F). (G–I) Zymosan evoked dose-dependent wiping (H) but not scratching behavior (G), and the wiping was dramatically reduced in TLR2 mice (I). N = 5–7 for each group. *P < 0.05; **P < 0.01; ***P < 0.001.

histamine-dependent itching (Shim and Oh, 2008; Imamachi et al., 2009), TRPA1 is vital for histamine-independent itches elicited by chloroquine, BAM8-22 and MrgprC11 (Wilson et al., 2011). TRPV1-expressing nociceptors are required for both histamine-dependent and histamine-independent itching (Imamachi et al., 2009). Based on our current study, we presume that the TLR2-induced pain and itch responses are mediated by TRPV1 and TRPA1 channels. First, TLR2 was coexpressed with TRPV1- and TRPA1-positive neurons. Second, TLR2 agonists increased the expression of TRPV1 and TRPA1 mRNA in TG neurons. Third, the pain and itch behaviors induced by the three TLR2 agonists were significantly reduced in both TRPV1 and TRPA1 KO mice. Finally, the TLR2 agonists Pam3CSK4 and zymosan dramatically increased the $[Ca^{2+}]_i$ in DRG neurons of WT mice, but this increased calcium influx

was largely inhibited in TRPV1 and TRPA1 KO mice. These results suggest that TLR2 participates in the regulation of pain and itching by regulating downstream TRPA1 and TRPV1 channels. However, the mechanisms by which the TLR2-induced modulation of TRPV1 and TRPA1 result in itching and pain still need to be investigated.

In conclusion, our study identified various types of neurons expressing TLR2 in the TG and DRG, demonstrated that TLR2 is involved in acute and chronic pain and itching, and revealed that different TLR2 agonists produce different pain and itch behaviors via downstream TRPV1 and TRPA1 signals by activating TLR1/TLR2 or TLR6/TLR2 heterodimers. This study provides a basis for elucidating the regulatory effects of TLR2 on itching and pain and for choosing different TLR2 agonists in TLR2 research and clinical treatments.

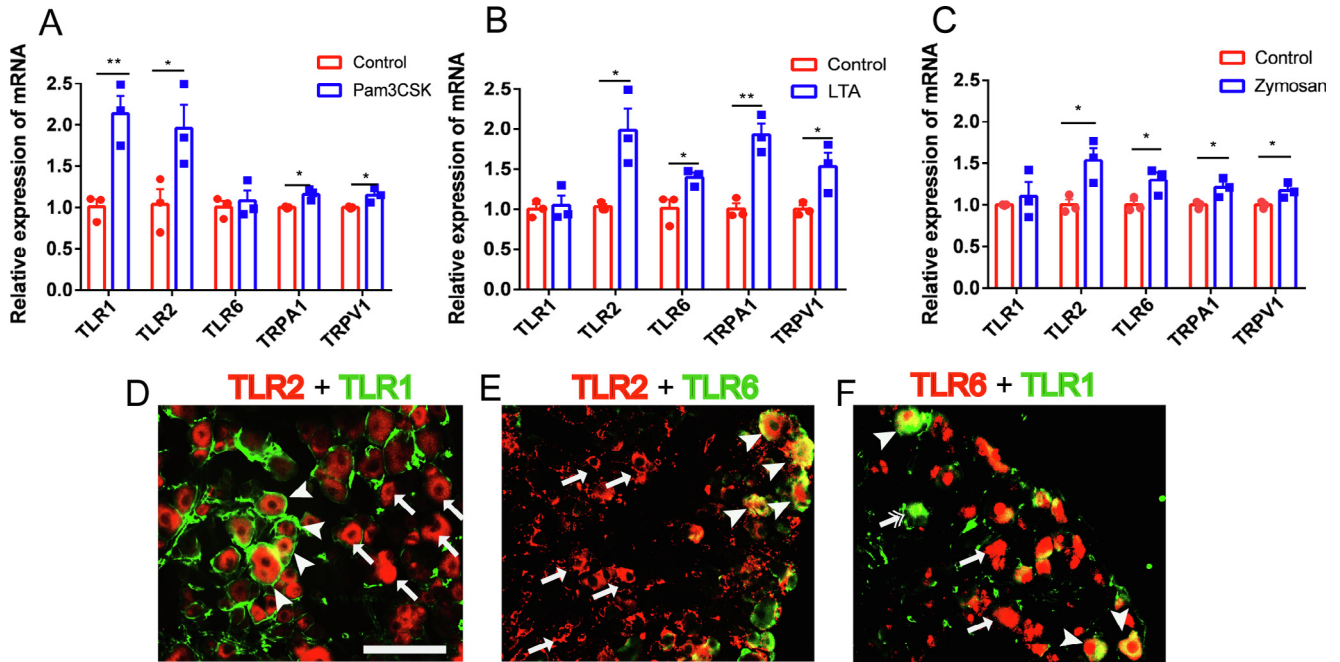


Fig. 6. Different TLR2 agonists increase the expression of different TLR2 mRNA heterodimers and the colocalization of TLR2 with TLR1 and TLR6 in TG or DRG neurons. (A–C) The TLR2, TRPV1 and TRPA1 mRNA expression levels were increased in the TG 30 min after the injection of Pam3CSK4, LTA and zymosan into the mouse cheek. Pam3CSK4 also increased the mRNA expression of TLR1 but not that of TLR6 in the TG (A); LTA (B) and zymosan (C) also increased the mRNA expression of TLR6 but not that of TLR1 in the TG. N = 3 for each group. *P < 0.05; **P < 0.01. (D–F) Colocalization of TLR2 with TLR1 (D), TLR2 with TLR6 (E) and TLR1 with TLR6 (F) in DRG neurons. The arrowheads in D and E indicate the colocalization of TLR2 with TLR1 or TLR6. The arrows in D and E indicate no TLR2 colocalization in DRG neurons. The arrowhead, arrow and double arrowhead in F indicate the colocalization of TLR1 with TLR6, TLR6 and TLR1, respectively. Bar = 50 μ m.

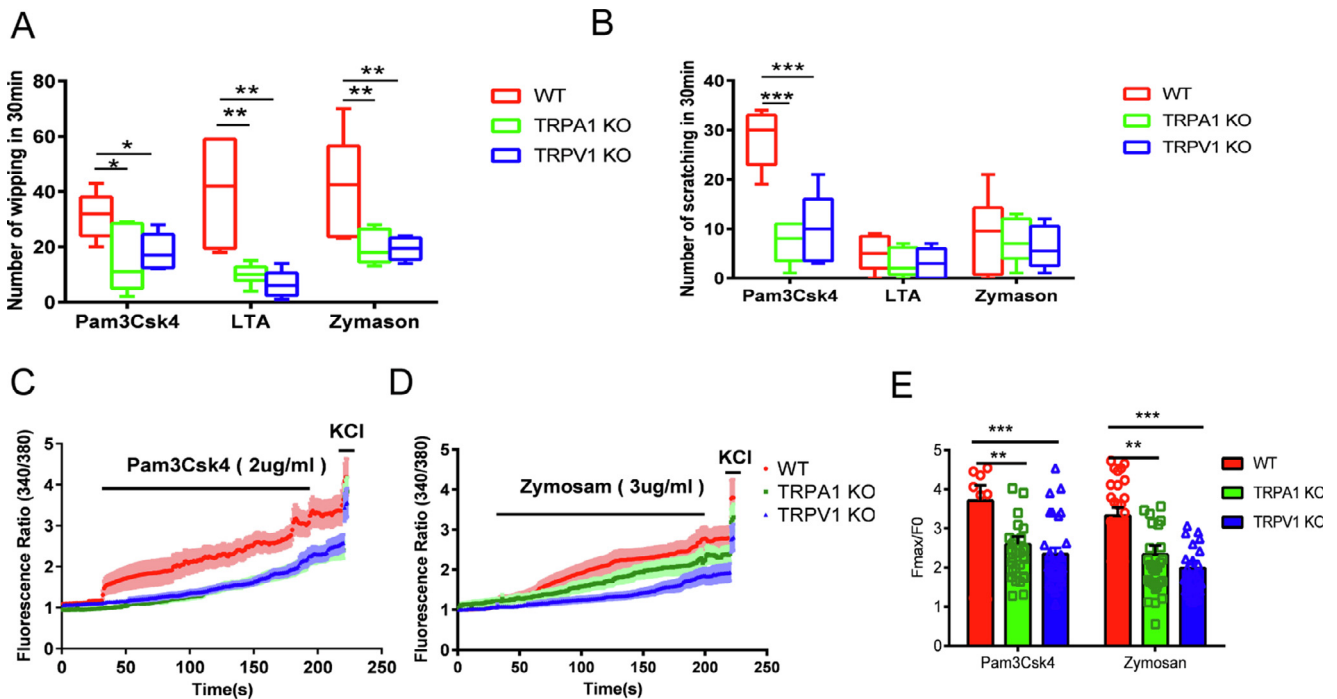


Fig. 7. Different TLR2 agonists evoke distinct nociceptive behaviors via TRPV1 and TRPA1. (A) Pam3CSK4, LTA and zymosan induced wipping in WT, TRPV1 and TRPA1 KO mice. (B) Pam3CSK4, LTA and zymosan induced scratching in WT, TRPV1 and TRPA1 KO mice. N = 5–7 for each group. *P < 0.05; **P < 0.01. ***P < 0.001. One-way ANOVA followed by a Fisher post hoc test. (C–F) The time-dependent [Ca²⁺]_i increases in DRG neurons induced by Pam3CSK4 (2 μ g/ml) (C) and zymosan (3 μ g/ml) (D) in WT, TRPV1 KO and TRPA1 KO mice. (E) F₀/F_{max} of [Ca²⁺]_i induced by Pam3CSK4 and zymosan in DRG neurons from WT, TRPA1KO and TRPV1KO mice. **P < 0.01 ***P < 0.001; one-way ANOVA followed by Bonferroni’s post hoc test. Thirty neurons from 3 mice were analyzed for each group.

CONFLICTS OF INTEREST

All authors have no conflicts of interest to declare.

ACKNOWLEDGMENTS

We thank Prof. Xin-Ming Jia and Prof. Xiao-Ping Chen of Tongji University for the TLR2 KO mice. We also thank Prof. Zhen-Zhong Xu of Zhe-Jiang University for the TRPV1 and TRPA1 KO mice. This work was supported by the National Natural Science Foundation of China (31271182), the National Key R&D Program of China (2019YFA0110300) and Shanghai Changning District Committee of Science and Technology of China (CNKW2018Y08).

REFERENCES

- Akira S, Uematsu S, Takeuchi O (2006) Pathogen recognition and innate immunity. *Cell* 124:783–801.
- Akiyama T, Carstens E (2013) Neural processing of itch. *Neuroscience* 250:697–714.
- Alexopoulou L, Thomas V, Schnare M, Lobet Y, Anguita J, Schoen RT, Medzhitov R, Fikrig E, Flavell RA (2002) Hyporesponsiveness to vaccination with *Borrelia burgdorferi* OspA in humans and in TLR1- and TLR2-deficient mice. *Nat Med* 8:878–884.
- Bruno K, Woller SA, Miller YI, Yaksh TL, Wallace M, Beaton G, Chakravarthy K (2018) Targeting toll-like receptor-4 (TLR4)-an emerging therapeutic target for persistent pain states. *Pain* 159:1908–1915.
- Chaplan SR, Bach FW, Pogrel JW, Chung JM, Yaksh TL (1994) Quantitative assessment of tactile allodynia in the rat paw. *J Neurosci Methods* 53:55–63.
- Christianson CA, Dumlao DS, Stokes JA, Dennis EA, Svensson CI, Corr M, Yaksh TL (2011) Spinal TLR4 mediates the transition to a persistent mechanical hypersensitivity after the resolution of inflammation in serum-transferred arthritis. *Pain* 152:2881–2891.
- Huang K, Hu DD, Bai D, Wu ZY, Chen YY, Zhang YJ, Lv X, Wang QX, Zhang L (2018) Persistent extracellular signal-regulated kinase activation by the histamine H4 receptor in spinal neurons underlies chronic itch. *J Invest Dermatol* 138:1843–1850.
- Hyunjung Min HL, Lim Hyounsub, Jang Yong Ho, Chung Sung Jun, Justin Lee C, Lee Sung Joong (2014) TLR4 enhanced histamine induced itch by TRPV1. *Mol Brain*.
- Ichikawa H, Matsuo S, Silos-Santiago I, Jacquin MF, Sugimoto T (2004) The development of myelinated nociceptors is dependent upon trks in the trigeminal ganglion. *Acta Histochem* 106:337–343.
- Imamachi N, Park GH, Lee H, Anderson DJ, Simon MI, Basbaum AI, Han SK (2009) TRPV1-expressing primary afferents generate behavioral responses to pruritogens via multiple mechanisms. *Proc Natl Acad Sci USA* 106:11330–11335.
- Ionescu MA, Baroni A, Brambilla L, Cannavo SP, Cristaudo A, Vedove CD, Frasca M, Girolomoni G, Gnecci L, Peris K, Trifiro C, Matta AM, Robert G (2011) Double blind clinical trial in a series of 115 patients with seborrheic dermatitis: prevention of relapses using a topical modulator of Toll like receptor 2. *G Ital Dermatol Venereol* 146:185–189.
- Jin MS, Kim SE, Heo JY, Lee ME, Kim HM, Paik SG, Lee H, Lee JO (2007) Crystal structure of the TLR1-TLR2 heterodimer induced by binding of a tri-acylated lipopeptide. *Cell* 130:1071–1082.
- Kang JY, Lee JO (2011) Structural biology of the Toll-like receptor family. *Annu Rev Biochem* 80:917–941.
- Kang JY, Nan X, Jin MS, Youn SJ, Ryu YH, Mah S, Han SH, Lee H, Paik SG, Lee JO (2009) Recognition of lipopeptide patterns by Toll-like receptor 2-Toll-like receptor 6 heterodimer. *Immunity* 31:873–884.
- Kawai T, Akira S (2010) The role of pattern-recognition receptors in innate immunity: update on Toll-like receptors. *Nat Immunol* 11:373–384.
- Kawai T, Akira S (2011) Toll-like receptors and their crosstalk with other innate receptors in infection and immunity. *Immunity* 34:637–650.
- Kawano T, Eguchi S, Iwata H, Yamanaka D, Tateiwa H, Locatelli FM, Yokoyama M (2016) Effects and underlying mechanisms of endotoxemia on post-incisional pain in rats. *Life Sci* 148:145–153.
- Kim AY, Tang Z, Liu Q, Patel KN, Maag D, Geng Y, Dong X (2008) Pirt, a phosphoinositide-binding protein, functions as a regulatory subunit of TRPV1. *Cell* 133:475–485.
- Kim D, Kim MA, Cho IH, Kim MS, Lee S, Jo EK, Choi SY, Park K, Kim JS, Akira S, Na HS, Oh SB, Lee SJ (2007) A critical role of toll-like receptor 2 in nerve injury-induced spinal cord glial cell activation and pain hypersensitivity. *J Biol Chem* 282:14975–14983.
- Kim D, You B, Lim H, Lee SJ (2011a) Toll-like receptor 2 contributes to chemokine gene expression and macrophage infiltration in the dorsal root ganglia after peripheral nerve injury. *Mol Pain* 7:74.
- Kim SJ, Park GH, Kim D, Lee J, Min H, Wall E, Lee CJ, Simon MI, Lee SJ, Han SK (2011b) Analysis of cellular and behavioral responses to imiquimod reveals a unique itch pathway in transient receptor potential vanilloid 1 (TRPV1)-expressing neurons. *Proc Natl Acad Sci USA* 108:3371–3376.
- Lacagnina MJ, Watkins LR, Grace PM (2018) Toll-like receptors and their role in persistent pain. *Pharmacol Ther* 184:145–158.
- Lim H, Kim D, Lee SJ (2013) Toll-like receptor 2 mediates peripheral nerve injury-induced NADPH oxidase 2 expression in spinal cord microglia. *J Biol Chem* 288:7572–7579.
- Liu T, Berta T, Xu ZZ, Park CK, Zhang L, Lu N, Liu Q, Liu Y, Gao YJ, Liu YC, Ma Q, Dong X, Ji RR (2012a) TLR3 deficiency impairs spinal cord synaptic transmission, central sensitization, and pruritus in mice. *J Clin Invest* 122:2195–2207.
- Liu T, Gao YJ, Ji RR (2012b) Emerging role of Toll-like receptors in the control of pain and itch. *Neurosci Bull* 28:131–144.
- Liu T, Han Q, Chen G, Huang Y, Zhao LX, Berta T, Gao YJ, Ji RR (2016) Toll-like receptor 4 contributes to chronic itch, allodynia, and spinal astrocyte activation in male mice. *Pain* 157:806–817.
- Liu, T, Ji, RR, Toll-Like Receptors and Itch. In: Carstens, E., Akiyama, T., editors. *Itch: Mechanisms and Treatment*. Boca Raton (FL), 2014.
- Liu T, Xu ZZ, Park CK, Berta T, Ji RR (2010) Toll-like receptor 7 mediates pruritus. *Nat Neurosci* 13:1460–1462.
- Luo X, Huh Y, Bang S, He Q, Zhang L, Matsuda M, Ji RR (2019) Macrophage toll-like receptor 9 contributes to chemotherapy-induced neuropathic pain in male mice. *J Neurosci*.
- Moore C, Gupta R, Jordt SE, Chen Y, Liedtke WB (2018) Regulation of pain and itch by TRP channels. *Neurosci Bull* 34:120–142.
- Oliveira-Nascimento L, Massari P, Wetzler LM (2012) The role of TLR2 in infection and immunity. *Front Immunol* 3:79.
- Oosting M, Ter Hofstede H, Sturm P, Adema GJ, Kullberg BJ, van der Meer JW, Netea MG, Joosten LA (2011) TLR1/TLR2 heterodimers play an important role in the recognition of *Borrelia spirochetes*. *PLoS One* 6:e25998.
- Panzer R, Blobel C, Folster-Holst R, Proksch E (2014) TLR2 and TLR4 expression in atopic dermatitis, contact dermatitis and psoriasis. *Exp Dermatol* 23:364–366.
- Park CK, Xu ZZ, Berta T, Han Q, Chen G, Liu XJ, Ji RR (2014) Extracellular microRNAs activate nociceptor neurons to elicit pain via TLR7 and TRPA1. *Neuron* 82:47–54.
- Qi J, Buzas K, Fan H, Cohen JI, Wang K, Mont E, Klinman D, Oppenheim JJ, Howard OM (2011) Painful pathways induced by TLR stimulation of dorsal root ganglion neurons. *J Immunol* 186:6417–6426.
- Ruscheweyh R, Forsthuber L, Schoffnegger D, Sandkuhler J (2007) Modification of classical neurochemical markers in identified primary afferent neurons with Abeta-, Adelta-, and C-fibers after chronic constriction injury in mice. *J Comp Neurol* 502:325–336.
- Sakamoto M, Asahina R, Kamishina H, Maeda S (2016) Transcription of thymic stromal lymphopoietin via Toll-like receptor 2 in canine keratinocytes: a possible association of *Staphylococcus* spp. in

- the deterioration of allergic inflammation in canine atopic dermatitis. *Vet Dermatol* 27:184–e46.
- Shim WS, Oh U (2008) Histamine-induced itch and its relationship with pain. *Mol Pain* 4:29.
- Shimada SG, LaMotte RH (2008) Behavioral differentiation between itch and pain in mouse. *Pain* 139:681–687.
- Takeda K, Takeuchi O, Akira S (2002) Recognition of lipopeptides by Toll-like receptors. *J Endotoxin Res* 8:459–463.
- Takeuchi O, Akira S (2001) Toll-like receptors; their physiological role and signal transduction system. *Int Immunopharmacol* 1:625–635.
- Takeuchi O, Sato S, Horiuchi T, Hoshino K, Takeda K, Dong Z, Modlin RL, Akira S (2002) Cutting edge: role of Toll-like receptor 1 in mediating immune response to microbial lipoproteins. *J Immunol* 169:10–14.
- Taves S, Ji RR (2015) Itch control by Toll-like receptors. *Handb Exp Pharmacol* 226:135–150.
- Towne C, Pertin M, Beggah AT, Aebischer P, Decosterd I (2009) Recombinant adeno-associated virus serotype 6 (rAAV2/6)-mediated gene transfer to nociceptive neurons through different routes of delivery. *Mol Pain* 5:52.
- Triantafilou M, Gamper FG, Haston RM, Mouratis MA, Morath S, Hartung T, Triantafilou K (2006) Membrane sorting of toll-like receptor (TLR)-2/6 and TLR2/1 heterodimers at the cell surface determines heterotypic associations with CD36 and intracellular targeting. *J Biol Chem* 281:31002–310011.
- Triantafilou M, Uddin A, Maher S, Charalambous N, Hamm TS, Alsumaiti A, Triantafilou K (2007) Anthrax toxin evades Toll-like receptor recognition, whereas its cell wall components trigger activation via TLR2/6 heterodimers. *Cell Microbiol* 9:2880–2892.
- Vaisid T, Kosower NS (2013) Calpastatin is upregulated in non-immune neuronal cells via toll-like receptor 2 (TLR2) pathways by lipid-containing agonists. *Biochim Biophys Acta* 1833:2369–2377.
- Wadachi R, Hargreaves KM (2006) Trigeminal nociceptors express TLR-4 and CD14: a mechanism for pain due to infection. *J Dent Res* 85:49–53.
- Wilson SR, Gerhold KA, Bifulck-Fisher A, Liu Q, Patel KN, Dong X, Bautista DM (2011) TRPA1 is required for histamine-independent, Mas-related G protein-coupled receptor-mediated itch. *Nat Neurosci* 14:595–602.
- Wu Z, Wang S, Wu I, Mata M, Fink DJ (2015) Activation of TLR-4 to produce tumour necrosis factor-alpha in neuropathic pain caused by paclitaxel. *Eur J Pain* 19:889–898.
- Xu ZZ, Kim YH, Bang S, Zhang Y, Berta T, Wang F, Oh SB, Ji RR (2015) Inhibition of mechanical allodynia in neuropathic pain by TLR5-mediated A-fiber blockade. *Nat Med* 21:1326–1331.
- Yamamoto M, Sato S, Mori K, Hoshino K, Takeuchi O, Takeda K, Akira S (2002) Cutting edge: a novel Toll/IL-1 receptor domain-containing adapter that preferentially activates the IFN-beta promoter in the Toll-like receptor signaling. *J Immunol* 169:6668–6672.
- Zahringer U, Lindner B, Inamura S, Heine H, Alexander C (2008) TLR2 - promiscuous or specific? A critical re-evaluation of a receptor expressing apparent broad specificity. *Immunobiology* 213:205–224.
- Zhang L, Jiang GY, Song NJ, Huang Y, Chen JY, Wang QX, Ding YQ (2014) Extracellular signal-regulated kinase (ERK) activation is required for itch sensation in the spinal cord. *Mol Brain* 7:25.
- Zhang ZJ, Guo JS, Li SS, Wu XB, Cao DL, Jiang BC, Jing PB, Bai XQ, Li CH, Wu ZH, Lu Y, Gao YJ (2018) TLR8 and its endogenous ligand miR-21 contribute to neuropathic pain in murine DRG. *J Exp Med* 215:3019–3037.
- Zhou FM, Cheng RX, Wang S, Huang Y, Gao YJ, Zhou Y, Liu TT, Wang XL, Chen LH, Liu T (2017) Antioxidants Attenuate Acute and Chronic Itch: Peripheral and Central Mechanisms of Oxidative Stress in Pruritus. *Neurosci Bull* 33:423–435.

(Received 8 August 2019, Accepted 7 January 2020)
(Available online 16 January 2020)